Contribution from the Department of Chemistry and Laboratory for Molecular Structure and Bonding, Texas A&M University, College Station, Texas 77843

Chemistry of $Rh_2(CO)_2Cl_2(dppm)_2$ and Compounds Derived Therefrom: Structural Characterization of $Rh_2(CO)Cl_4(dppm)_2$ and $[Rh_2(CO)Cl_3(dppm)_2MeOH][PF_6]$

F. Albert Cotton,* Cassandra T. Eagle, and Andrew C. Price

Received May 24, 1988

$Rh_2(CO)_2Cl_2(dppm)_2$ (dppm = $(Ph_2P)_2CH_2$) reacts with 1 equiv of $PhICl_2$ in a dilute CH_2Cl_2 solution to yield $Rh_2(CO)_2Cl_4(dppm)_2$ (**1**), which was characterized in solution by IR and $^{31}P\{^1H\}$ NMR spectroscopies. $Rh_2(CO)_2Cl_4(dppm)_2$ slowly decarbonylates in solution, or more rapidly in the presence of an additional 1 equiv of $PhICl_2$, to give $Rh_2(CO)Cl_4(dppm)_2$ (**2**), which was characterized by X-ray crystallography. Compound **2** crystallizes in the space group *Cc*; the cell dimensions are a = 19.550 (7) Å, b = 16.872 (4) Å, c = 17.458 (4) Å, β = 107.29 (2)°, V = 5498 (3) Å^3, and Z = 4. The reaction of **2** with CO gives back $Rh_2(CO)_2Cl_4(dppm)_2$ while with 1 equiv of $PhICl_2$ it yields $Rh_2Cl_6(dppm)_2$ (**3**). Compound **2** further reacts with 1 equiv of $AgPF_6$ to give $[Rh_2(CO)Cl_3(dppm)_2MeOH][PF_6]$ (**4**), which was characterized by IR (solution and solid) and $^{31}P\{^1H\}$ NMR spectroscopies and by X-ray crystallography. Compound **4** crystallizes in the space group $P2_12_12_1$; the cell dimensions are a = 19.577 (6) Å, b = 27.040 (7) Å, c = 10.533 (2) Å, V = 5576 (2) Å^3, and Z = 4. The CO ligand may be removed from **2** with Me_3NO to give $Rh_2Cl_4(dppm)_2$ (**5**), a previously reported compound in which the dppm ligands are in a cisoid arrangement about the metal atoms. Conversely, $Rh_2Cl_4(dppm)_2$ reacts with CO under pressure to yield **2**. Direct chlorination of **5** to give **3** has not been accomplished.

Introduction

Halogenation and metathesis reactions of $Rh_2(CO)_2Cl_2(dppm)_2$ (dppm = $(Ph_2P)_2CH_2$) involving iodine and bromine are well-known. The metathesis of $Rh_2(CO)_2Cl_2(dppm)_2$, with Br^- leads to a complex with an "A-frame" structure, $[Rh_2(\mu\text{-}CO)Br_2(dppm)_2]$,[1,2] the chloro analogue of which was prepared by refluxing $Rh_2(CO)_2Cl_2(dppm)_2$ in toluene.[2] Oxidative addition of iodine to $Rh_2(CO)_2Cl_2(dppm)_2$ gives $Rh_2(CO)_2Cl_2(I)_2(dppm)_2$.[3] Until recently, chlorination reactions of $Rh_2(CO)_2Cl_2(dppm)$ have led only to a variety of uncharacterized products, probably because of the difficulty of quantitatively monitoring gaseous chlorine.[4] A recent report has shown that $Rh_2(CO)_2Cl_2(dppm)_2$ can be electrochemically oxidized in the presence of a chloride ion source.[4] This report indicates that the primary product from such oxidations is $Rh_2(CO)Cl_4(dppm)_2$, which upon workup with MeOH in the presence of $[NBu_4][PF_6]$, (the background electrolyte) gives rise to a product formulated as $[Rh_2(CO)Cl_3(dppm)_2][PF_6]$. The products of the electrochemical studies were not subjected to crystallographic analysis.

We report here the reactions of $Rh_2(CO)_2Cl_2(dppm)_2$ with stoichiometric amounts of $PhICl_2$[7] (a solid chlorine equivalent). We have found that we can cleanly synthesize and identify compounds along the path leading ultimately to the synthesis of a highly oxidized Rh_2^{6+} product with six chloride and no carbonyl ligands, $Rh_2Cl_6(dppm)_2$ (**3**). We report the synthesis and characterization of $Rh_2(CO)_2Cl_4(dppm)_2$ (**1**), $Rh_2(CO)Cl_4(dppm)_2$ (**2**), $Rh_2Cl_6(dppm)_2$ (**3**), and $[Rh_2(CO)Cl_3(dppm)_2MeOH][PF_6]$ (**4**). All of these products were characterized by IR and $^{31}P\{^1H\}$ NMR spectroscopies; **2** and **4** were further characterized by X-ray crystallography. The relationships among the previously known and the new compounds are summarized in Scheme I.

Note Added In Proof: Since the submission of this article, the crystal structure of the bis(dimethylphosphino)methane (dmpm) analogue of compound **1**, i.e. $Rh_2(CO)_2Cl_4(dmpm)_2$, has been published: Jenkins, J. A.; Ennett, J. P.; Cowie, M. *Organometallics* **1988**, *7*, 1845. The structure of the molecule is exactly analogous to our proposed structure for **1** as shown in Scheme I.

Experimental Section

General literature methods were used to prepare $Rh_2(CO)_2Cl_2(dppm)_2$,[5] $Rh_2Cl_4(dppm)_2$,[6] and $PhICl_2$.[7] Me_3NO (Aldrich) was sublimed prior to use, and $AgPF_6$ (Strem) was used as supplied. Silica gel was purchased from ICN (0.032-0.063 mm, d = 0.4 g/mL). All manipulations, unless otherwise stated, were done under an argon atmosphere using standard vacuum-line techniques. Infrared spectra were recorded on Perkin-Elmer 783 and IBM Instruments IR/44 Fourier Transform spectrometers by using either Nujol mulls between CsI plates or CH_2Cl_2 solutions in cells with NaCl plates. $^{31}P\{^1H\}$ NMR and $^{13}C\{^1H\}$ NMR spectra were recorded on an XL-200 Varian spectrometer at 81 and 50 MHz, respectively. Chemical shifts for $^{31}P\{^1H\}$ NMR spectra were referenced to external 85% H_3PO_4; more positive values represent deshielding. A trace of $CDCl_3$ was added to solutions for $^{13}C\{^1H\}$ NMR spectroscopy so that the carbon atom of this solvent could be used as a reference. Microanalyses were performed by Galbraith Laboratories, Inc., Knoxville, TN.

Reactions of $Rh_2(CO)_2Cl_2(dppm)_2$ with $PhICl_2$. Preparation of $Rh_2(CO)_2Cl_4(dppm)_2$ (1). To a slurry of 0.20 g (1.82×10^{-4} mol) of $Rh_2(CO)_2Cl_2(dppm)_2$, in 120 mL of CH_2Cl_2, was added $PhICl_2$ (50 mg, 0.18 mmol) in two portions over 10 min. The complex slowly dissolved over the course of 2 h to give an orange-brown solution. This solution initially exhibited three carbonyl peaks in the solution IR spectrum: 2047 cm^{-1} for **1**, 2023 cm^{-1} for $Rh_2(CO)Cl_4(dppm)_2$ (**2**, vide infra), and 1990 cm^{-1} for unreacted $Rh_2(CO)_2Cl_2(dppm)_2$. After 5 h the ν_{CO} mode at 2023 cm^{-1} for **2** was the only band remaining. Evidently, the dicarbonyl $Rh_2(CO)_2Cl_4(dppm)_2$ (**1**) decarbonylates in solution to form the monocarbonyl $Rh_2(CO)Cl_4(dppm)_2$ (**2**). A solid sample of **1** was prepared by bubbling CO through a CH_2Cl_2 solution of **2** (0.10 g in 20 mL) for 5 min. The solution quickly changed from brown to orange. The product was precipitated upon addition of 60 mL of hexane while under an atmosphere of CO. The precipitate was then filtered off and dried under reduced pressure. The yield is quantitative. IR (CH_2Cl_2 solution): 2047 cm^{-1}. IR (Nujol mull): 2023 cm^{-1}. The $^{31}P\{^1H\}$ NMR spectrum (CH_2Cl_2 solution under a CO atmosphere) showed an AA'A''A'''XX' pattern centered at 9.20 ppm, $^xJ_{Rh-P}$ = 104.9 Hz. The data are in close agreement with those reported by Woods et al.[4]

Preparation of $Rh_2(CO)Cl_4(dppm)_2$ (2). Method 1. The CH_2Cl_2 solution of $Rh_2(CO)_2Cl_4(dppm)_2$ from above was stirred under argon for 10 h. At the end of this time, the solution showed only one carbonyl stretching frequency of ν = 2023 cm^{-1} (s) in the IR spectrum. The solution was concentrated to ca. 10 mL and separated from trace amounts of $Rh_2(CO)_2Cl_4(dppm)_2$ and $Rh_2Cl_6(dppm)_2$ by column chromatography,[8] employing a 2.5-cm-diameter column packed with 16 cm of silica and eluted with a 6:1 mixture of $CHCl_3$-MeOH. The second fraction, namely **2**, was collected, and the solvents were removed by vacuum distillation. The dark orange residue was redissolved in a small volume of CH_2Cl_2 and then treated with a large excess of hexane to precipitate the desired product. This precipitate was filtered off and dried under reduced pressure. Yield: 0.470 g, 90%. $^{31}P\{^1H\}$ NMR: Complex AA'BB' pattern: δ_1 = 8.1; δ_2 = 10.9. IR (CH_2Cl_2 solution): 2023 cm^{-1}. IR (Nujol mull): 2022 (s), 1575 (m), 1440 (s), 1195 (m), 1165 (m), 1100 (s), 1035 (m), 1005 (m), 980 (w), 900 (w), 855 (w), 780 (s), 745 (s), 735 (s), 700 (s), 555 (m), 530 (s), 520 (s), 495 (m) cm^{-1}. Orange-brown X-ray quality crystals were grown from a CH_2Cl_2 solution of $Rh_2(CO)Cl_4(dppm)_2$ layered with C_6H_6.

Preparation of $Rh_2(CO)Cl_4(dppm)_2$. Method 2. $Rh_2(CO)_2Cl_2(dppm)_2$ (0.20 g, 1.82×10^{-4} mol) was slurried in 150 mL of CH_2Cl_2. $PhICl_2$

(1) Cowie, M.; Dwight, S. K. *Inorg. Chem.* **1980**, *19*, 2508.
(2) Cowie, M.; Dwight, S. K. *Inorg. Chem.* **1980**, *19*, 2500.
(3) Balch, A. L.; Tulyathan, B. *Inorg. Chem.* **1977**, *16*, 2840.
(4) Tortorelli, L. J.; Tinsley, P. W.; Woods, C.; Janke, C. J. *Polyhedron* **1988**, *7*, 315.
(5) Mague, J. T.; Mitchner, J. P. *Inorg. Chem.* **1969**, *8*, 119.
(6) Cotton, F. A.; Dunbar, K. R.; Verbruggen, M. G. *J. Am. Chem. Soc.* **1987**, *109*, 5498.
(7) Lucas, H. J.; Kennedy, E. R. *Org. Synth.* **1955**, *3*, 482.
(8) Still, W. C.; Kahn, M.; Mitra, A. *J. Org. Chem.* **1978**, *43*, 2923.

0020-1669/88/1327-4362$01.50/0

Scheme I

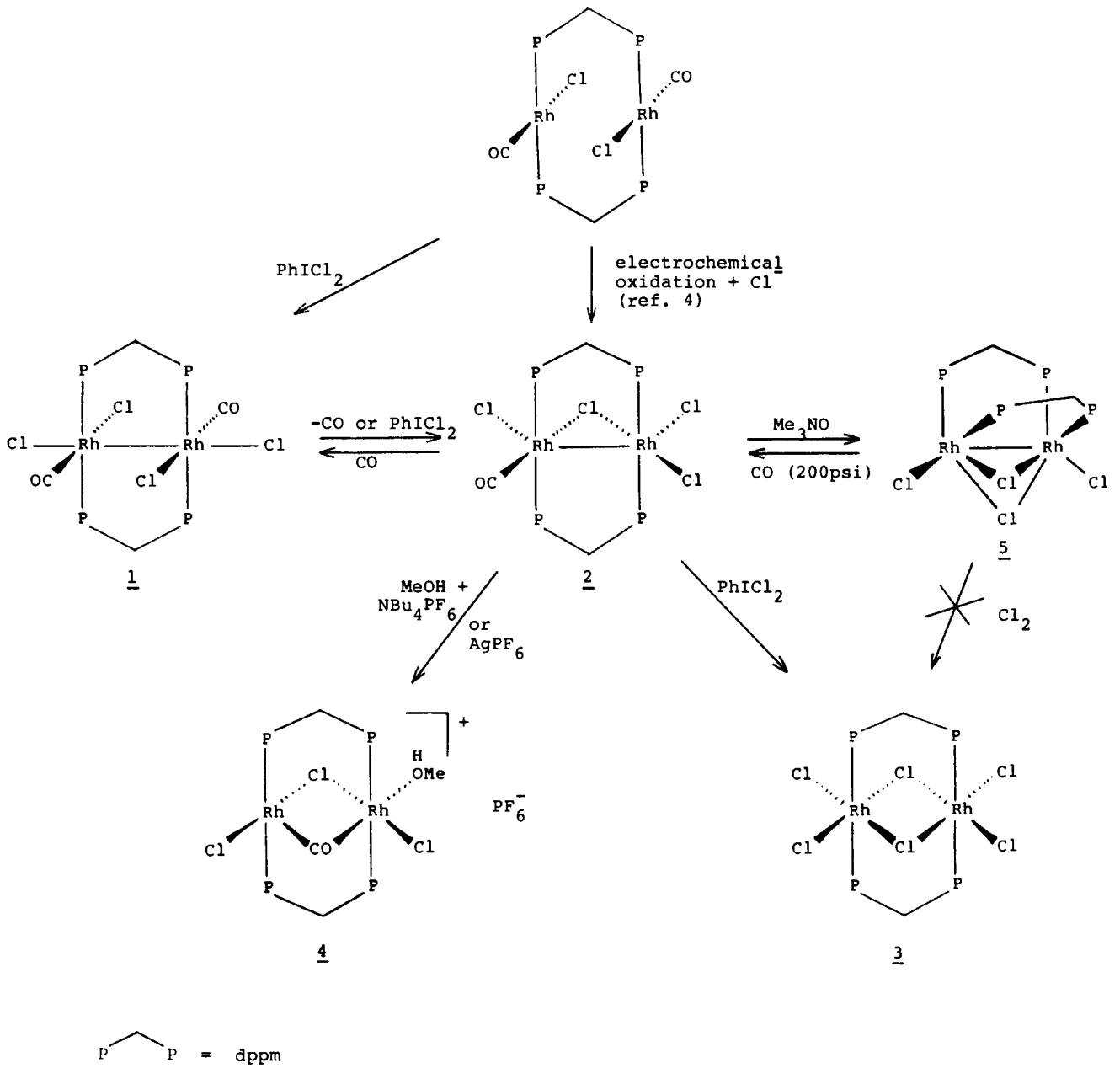

(0.050 g, 1 eq) was added, and after 24 h another 0.050 g was added. Stirring was continued for an additional 6 h. The resulting brown solution was concentrated to ca. 10 mL and purified by column chromatography (see above). Yield of $Rh_2(CO)Cl_4(dppm)_2$ (second fraction): 0.109 g, 52%. Yield of $Rh_2Cl_6(dppm)_2$ (first fraction): 0.082 g, 38%.

Preparation of $Rh_2Cl_6(dppm)_2$ (3). $Rh_2(CO)_2Cl_2(dppm)_2$ (0.25 g, 2.27 × 10^{-4} mol) was stirred in 300 mL of CH_2Cl_2. $PhICl_2$ (0.187 g, 3 equiv) was added over a period of 72 h (1 equiv/24 h). The resulting pale orange solution was evaporated to dryness by vacuum distillation, and the solid residue was redissolved in 5 mL of CH_2Cl_2. An excess of benzene was added to yield a yellow precipitate. This was filtered off and dried under reduced pressure. Yield: 0.23 g, 84%. No carbonyl stretching frequency was observed in either the Nujol mull or the solution IR spectra. The $^{31}P\{^1H\}$ NMR spectrum shows an essentially AX pattern centered at δ = 4.65, $^1J_{Rh-P}$ = 85.5 Hz. IR (Nujol mull): 2720 (w), 1730 (w), 1700 (w), 1570 (w), 1435 (s), 1310 (w), 1275 (w), 1195 (w), 1165 (w), 1095 (m), 1075 (w), 1035 (w), 1005 (w), 780 (s), 740 (s), 715 (m), 695 (s), 690 (s), 530 (m), 515 (w), 490 (m), 470 (w), 425 (w), 385 (m), 355 (m) cm^{-1}.

Reactions of $Rh_2(CO)Cl_4(dppm)_2$. (a) MeOH. MeOH (5 mL) was added to a CH_2Cl_2 solution of $Rh_2(CO)Cl_4(dppm)_2$ (0.020 g in 2 mL of CH_2Cl_2). The resulting green solution was analyzed by $^{31}P\{^1H\}$ NMR spectroscopy: δ = 10.3, $^xJ_{Rh-P}$ = 94.6 Hz. The AA'A''A'''XX' pattern is indicative of the formation of $[Rh_2(CO)Cl_3(dppm)_2][Cl]$.[4] The solvent was evaporated to re-form $Rh_2(CO)Cl_4(dppm)_2$ (as analyzed by IR and $^{31}P\{^1H\}$ NMR spectroscopies). The reaction was quantitative.

(b) $AgPF_6$. $AgPF_6$ (0.043 mg, 1.7 × 10^{-4} mol) was dissolved in 20 mL of CH_2Cl_2. This was added to a rapidly stirred solution of $Rh_2(CO)Cl_4(dppm)_2$ (0.194 g in 30 mL of CH_2Cl_2). Immediately, a clear green solution was formed along with a small amount of white precipitate. The solution was filtered to remove the precipitate (AgCl). The $^{31}P\{^1H\}$ spectrum of the solution, i.e., $[Rh_2(CO)Cl_3(dppm)_2][PF_6]$, exhibited an AA'A''A'''XX' pattern: δ = 13.6, $^xJ_{Rh-P}$ = 95.7 Hz; $\delta(PF_6)$ = −141.8, $^1J_{PF}$ = 711 Hz. IR (CH_2Cl_2 solution): 1790 cm^{-1}. IR (Nujol mull): 1789 (s), 1615 (m), 1591 (m), 1579 (m), 1490 (s), 1315 (m), 1265 (s), 1200 (m), 1152 (s), 1105 (s), 1035 (s), 1010 (s), 985 (w), 937 (w), 850 (br, s), 800 (m), 780 (s), 750 (s), 732 (s), 700 (s), 630 (m), 620 (s), 575 (s), 535 (s), 520 (s), 495 (m), 470 (w), 460 (w), 455 (w), 410 (w), 390 (w), 345 (s) cm^{-1}. Anal. Calcd. for $Rh_2Cl_3F_6P_5C_{53}H_{52}O_3$: C, 48.30, H, 3.98. Found: C, 47.12; H, 4.70. Green X-ray quality crystals of $[Rh_2(CO)Cl_3(dppm)_2MeOH][PF_6]$ (**4**) were grown from a CH_2Cl_2 solution of $[Rh_2(CO)Cl_3(dppm)_2][PF_6]$, layered with MeOH.

(c) BF_3·Et_2O. $Rh_2(CO)Cl_4(dppm)_2$ (0.0266 g, 2.33 × 10^{-5} mol) was dissolved in 5 mL of CH_2Cl_2, and then 3 μL of BF_3·Et_2O (1 equiv) was added. The solution color changed from brown to green within 5 min. $^{31}P\{^1H\}$ NMR: δ_P = 13.3 ppm, $^xJ_{Rh-P}$ = 93.8 Hz. IR (CH_2Cl_2 solution): 1785 cm^{-1}. The reaction occurs immediately if 1 mL of MeOH is added to the CH_2Cl_2 prior to BF_3·Et_2O addition.

(d) Me_3NO. Me_3NO (0.008 g, 1.07 × 10^{-4} mol) was added to a CH_2Cl_2 (25 mL) solution of $Rh_2(CO)Cl_4(dppm)_2$ (0.113 g, 1 equiv) at −72 °C. After 7 h, the reaction mixture was warmed to −10 °C. A gradual decrease in $Rh_2(CO)Cl_4(dppm)_2$, the corresponding formation

Table I. Crystal Data for $Rh_2(CO)Cl_4(dppm)_2 \cdot CH_2Cl_2 \cdot C_6H_6 \cdot H_2O$ and $[Rh_2(CO)Cl_3(dppm)_2MeOH]PF_6 \cdot MeOH$

formula	$Rh_2Cl_6P_4O_2C_{58}H_{54}$	$Rh_2Cl_3P_5F_6O_3C_{53}H_{52}$
fw	1325.49	1318.02
space group	*Cc*	$P2_12_12_1$
a, Å	19.550 (7)	19.577 (6)
b, Å	16.872 (4)	27.040 (7)
c, Å	17.458 (4)	10.533 (2)
β, deg	107.29 (2)	
V, Å^3	5498 (3)	5576 (2)
Z	4	4
d_{calcd}, g/cm^3	1.596	1.570
μ(Mo Kα), cm^{-1}	10.416	9.296
radiation (monochromated in incident beam)	Mo Kα (λ_α = 0.71073 Å)	
temp, °C	20 ± 2	20 ± 2
transmissn factors: max; min	1.0000; 0.7780	0.9995; 0.9447
R^a	0.0639	0.0636
R_w^b	0.0826	0.0832

$^a R = \sum||F_o| - |F_c||/\sum|F_o|$. $^b R_w = [\sum w(|F_o| - |F_c|)^2/\sum w|F_o|^2]^{1/2}$; $w = 1/\sigma^2(|F_o|)$.

of $Rh_2Cl_4(dppm)_2$ (**5**), and the gradual formation of a small amount of dppm oxide were observed by TLC and $^{31}P\{^1H\}$ NMR spectroscopy. After 53 h at −10 °C, the salmon-colored precipitate ($Rh_2Cl_4(dppm)_2$, **5**), was rapidly isolated by filtration, washed with MeOH, and dried in vacuo. Yield: 0.075 g, 68%. The IR and $^{31}P\{^1H\}$ NMR spectra of this compound were found to be the same as those of an authentic sample that was prepared via a different route.[6]

Test for Phosgene. The effluent gas from the preparation of $Rh_2(CO)Cl_4(dppm)_2$, method 2, was bubbled through MeOH (50 mL) in a flask protected from direct light. After 24 h, the volume of the MeOH was reduced via distillation to ca. 10 mL and analyzed by $^{13}C\{^1H\}$ NMR spectroscopy. No peaks attributable to $(MeO)_2CO$ were found.

Reaction of $Rh_2Cl_4(dppm)_2$ with CO. A 350-mL Parr bomb reactor was charged with a slurry of $Rh_2Cl_4(dppm)_2$ (0.050 g) in CH_2Cl_2 (100 mL). The reactor was pressurized with 200 psi of CO and stirred for 72 h. The solution was then concentrated to 10 mL and analyzed by $^{31}P\{^1H\}$ NMR spectroscopy: $Rh_2(CO)Cl_4(dppm)_2$, 51.3%; $Rh_2(CO)_2Cl_4(dppm)_2$, 35.2%; $Rh_2Cl_4(dppm)_2$, 10.4%; bis(diphenylphosphino)methane oxide, 3.1%. Percent yields were calculated from peak heights in the NMR spectrum.

Reactions of $Rh_2Cl_4(dppm)_2$ with Cl_2. (a) $PhICl_2$. $Rh_2Cl_4(dppm)_2$ (0.050 g) was refluxed with $PhICl_2$ (10 equiv) in $CHCl_3$ (50 mL) for 72 h. The starting material was recovered unchanged as analyzed by $^{31}P\{^1H\}$ NMR and IR spectroscopies. The same result was obtained when C_6H_6 was substituted for $CHCl_3$ in the above reaction.

(b) Cl_2 Gas. A slurry of $Rh_2Cl_4(dppm)_2$ (0.050 g) in CH_2Cl_2 (100 mL) was bubbled with Cl_2 gas for 5 h. The solution was concentrated to ca. 10 mL and analyzed by $^{31}P\{^1H\}$ NMR and IR spectroscopies. $Rh_2Cl_4(dppm)_2$ was the only compound detected.

(c) Cl_2 Liquid. A slurry of $Rh_2Cl_4(dppm)_2$ (0.050 g) in Cl_2 liquid (25 mL) was refluxed for 24 h (by using a column condenser cooled to −80 °C). The complex slowly dissolved, forming an orange-red solution. The Cl_2 was evaporated, the red-orange solid was dissolved in CH_2Cl_2 (5 mL), and the product was analyzed by $^{31}P\{^1H\}$ NMR spectroscopy. The broad, featureless hump at δ = 15 indicated that the product was paramagnetic (and therefore not $Rh_2Cl_6(dppm)_2$). Attempts to grow crystals of this product were unsuccessful.

X-ray Crystallography. The Structures of **2** and **4** were determined by general procedures fully described elsewhere.[9] Data reductions were carried out by standard methods using well-established computational procedures.[10] The crystal parameters and basic information pertaining to data collection and structure refinement are summarized in Table I. Tables II and III list the positional parameters for structures **2** and **4**, respectively. Selected bond distances and bond angles of **2** and **4** are found in Tables IV and V, respectively. Complete tables of crystal parameters, data collection, structure refinement, bond distances, and bond angles as well as anisotropic thermal parameters and structure factors are available as supplementary material.

$Rh_2(CO)Cl_4(dppm)_2$ (2). The direct-methods program in SHELXS-86[11] was used to locate the two independent rhodium atoms. The rest of the atoms were located and refined by using the SHELX-76 package.[12] The carbonyl ligand, which was located by using the first difference Fourier map, was refined with restrained bond distances: Rh(1)–C(1) = 1.800 (5) Å; Rh(1)–O(1) = 2.900 (5) Å; C(1)–O(1) = 1.100 (5) Å. This model allowed for refinement with the initial assumption that the Rh(1)–C(1)–O(1) bond angle = 180°. In the last stages of refinement, all bond distance restraints, except the one on C(1)–O(1), were removed. Three interstitial solvent molecules were found, CH_2Cl_2, H_2O, and C_6H_6. Four atoms of the benzene molecule were located, from which the locations of the other two were calculated. The benzene molecule was refined as a perfect hexagon. The highest peak in the final difference Fourier map, 1.006 e/Å^3, was associated with the benzene solvent molecule.[13]

$[Rh_2(CO)Cl_3(dppm)_2MeOH]PF_6$ (4). The SHELXS-86[11] direct methods program was used to locate the inner coordination sphere, from which the rest of the atoms were located by using the SHELX-76 package.[12] One interstial molecule of methanol per dirhodium species was also located from a difference Fourier map. After isotropic convergence, DIFABS[14] (an additional absorption correction) was applied. After subsequent anisotropic refinement, the alternative enantiomorph was tested but found to give a slightly higher *R* value. The highest peak in the final difference Fourier map (1.33 e/Å^3) was 0.7 Å from Rh(1) and therefore may be associated with a series termination error.

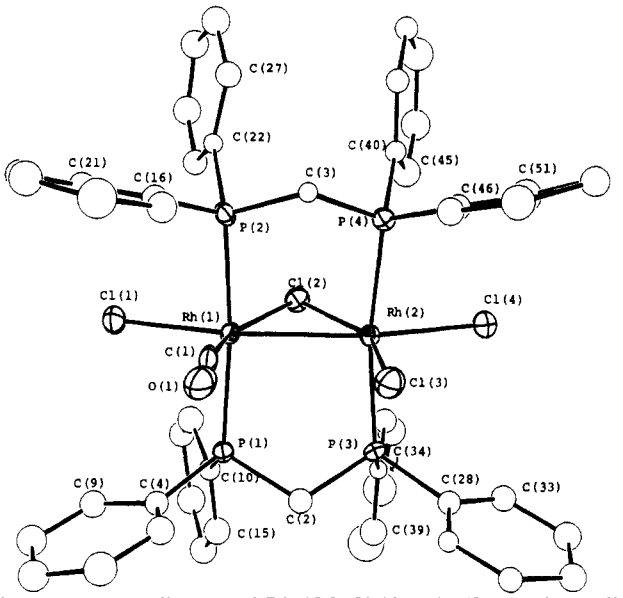

Figure 1. ORTEP diagram of $Rh_2(CO)Cl_4(dppm)_2$ (**2**) showing 30% probability ellipsoids. Two carbon atoms of each phenyl ring are labeled. Carbon atoms are numbered sequentially around the ring.

Discussion

Description of the Structure of $Rh_2(CO)Cl_4(dppm)_2$ (2). The ORTEP diagram of $Rh_2(CO)Cl_4(dppm)_2$ (Figure 1) reveals the structure of a dinuclear metal complex containing an M_2L_9 core and possessing an A-frame-type of structure. The A-frame is defined by the "A" formed from the O(1)–C(1)–Rh(1)–Cl(2)–Rh(2)–Cl(3) connectivity. Because of the presence of the additional atoms Cl(1) and Cl(4), we refer to this structure as an "A-frame-type" rather than simply as an A-frame.

The distance between the two independent rhodium atoms (2.691 (3) Å) corresponds to that of a rhodium–rhodium single bond. The Rh–Cl bonds are not all equivalent, suggesting the possibility of selective removal of chloride ligands.

(9) General procedures have been described. (a) Bino, A.; Cotton, F. A.; Fanwick, P. E.; *Inorg. Chem.* **1979**, *18*, 3558. (b) Cotton, F. A.; Frenz, B. A.; Deganello, G.; Shave, A. *J. Organomet. Chem.* **1973**, *50*, 227.
(10) Computing was done on a Local Area VAX Cluster, employing the VAX/VMS V4.6.
(11) Sheldrick, G. M. "SHELXS-86", Institut für Anorganische Chemie der Universität, Göttingen, FRG, 1986.
(12) Sheldrick, G. M. "SHELX-76", University of Cambridge, 1976.
(13) Air-stable crystals of $Rh_2(CO)Cl_4(dppm)_2$ can be formed by layering a $CHCl_3$ solution of the complex with Et_2O. Crystals grow in the tetragonal space group $P4_12_12_1$: a = 14.888 (3) Å, b = 14.888 (3) Å, c = 25.772 (3) Å, V = 5712 (1) Å^3. The crystallographically imposed C_2 axis allows for disorder between the CO ligand and Cl(3). This structure was solved with SHELX-76 by fixing occupancy factors of the CO and Cl(3) ligands and bond distances of these ligands to the rhodium. Since $Rh_2(CO)Cl_4(dppm)_2$ also crystallizes in *Cc*, we chose to report the undisordered model.
(14) Walker, N.; Stuart, D. *Acta Crystallogr., Sect. A: Found. Crystallogr.* **1983**, *39*, 158.

Table II. Positional Parameters and Equivalent Isotropic Thermal Parameters and Their Estimated Standard Deviations for $Rh_2(CO)Cl_4(dppm)_2 \cdot CH_2Cl_2 \cdot C_6H_6 \cdot H_2O$

atom	x	y	z	B,[a] Å²	atom	x	y	z	B,[a] Å²
Rh(1)	0.516	0.1846 (1)	0.423	2.13 (5)	C(26)	0.395 (2)	−0.062 (2)	0.595 (2)	4.6 (9)
Rh(2)	0.5126 (1)	0.2998 (1)	0.5279 (2)	2.09 (5)	C(27)	0.453 (2)	−0.018 (1)	0.592 (2)	4.2 (9)
Cl(1)	0.4750 (4)	0.0863 (4)	0.3155 (4)	3.5 (2)	C(28)	0.560 (1)	0.491 (1)	0.483 (1)	2.3 (6)
Cl(2)	0.4087 (3)	0.2343 (4)	0.4430 (4)	3.0 (1)	C(29)	0.635 (1)	0.499 (1)	0.494 (1)	2.2 (5)
Cl(3)	0.6385 (4)	0.3189 (5)	0.5738 (4)	4.2 (2)	C(30)	0.673 (1)	0.560 (2)	0.535 (2)	3.4 (6)
Cl(4)	0.4708 (5)	0.3963 (4)	0.6071 (5)	4.8 (2)	C(31)	0.637 (2)	0.622 (2)	0.566 (1)	4.0 (8)
P(1)	0.5189 (5)	0.2771 (4)	0.3220 (5)	2.5 (2)	C(32)	0.563 (2)	0.614 (2)	0.554 (2)	4.3 (6)*
P(2)	0.5288 (4)	0.0831 (4)	0.5178 (5)	2.5 (2)	C(33)	0.526 (1)	0.547 (2)	0.515 (2)	3.6 (6)*
P(3)	0.5109 (4)	0.4037 (4)	0.4384 (5)	2.1 (2)	C(34)	0.428 (1)	0.449 (1)	0.379 (1)	2.0 (5)
P(4)	0.5268 (4)	0.2126 (4)	0.6351 (4)	2.2 (2)	C(35)	0.360 (1)	0.429 (2)	0.390 (2)	3.9 (8)
O(1)	0.671 (2)	0.169 (1)	0.455 (2)	6.0 (8)	C(36)	0.301 (2)	0.463 (2)	0.346 (3)	7 (1)
C(1)	0.613 (2)	0.169 (2)	0.441 (2)	4.1 (9)	C(37)	0.299 (2)	0.516 (3)	0.288 (2)	7 (1)
C(2)	0.553 (1)	0.376 (2)	0.362 (2)	3.4 (5)*	C(38)	0.368 (2)	0.536 (2)	0.272 (3)	7 (1)*
C(3)	0.571 (1)	0.123 (1)	0.620 (1)	2.2 (4)*	C(39)	0.430 (2)	0.504 (2)	0.318 (2)	4.4 (6)*
C(4)	0.577 (1)	0.248 (2)	0.263 (2)	3.8 (8)	C(40)	0.450 (1)	0.182 (2)	0.661 (1)	2.9 (6)
C(5)	0.652 (1)	0.257 (2)	0.292 (2)	4.0 (8)	C(41)	0.455 (1)	0.127 (2)	0.722 (2)	3.5 (5)*
C(6)	0.699 (2)	0.228 (2)	0.254 (2)	6 (1)	C(42)	0.392 (1)	0.100 (2)	0.741 (1)	3.2 (7)
C(7)	0.665 (2)	0.190 (2)	0.178 (2)	5 (1)	C(43)	0.331 (2)	0.137 (2)	0.705 (2)	4.7 (7)*
C(8)	0.588 (2)	0.177 (2)	0.146 (2)	4.7 (7)*	C(44)	0.324 (2)	0.201 (2)	0.648 (2)	4.3 (6)*
C(9)	0.547 (2)	0.206 (2)	0.194 (2)	4.0 (6)*	C(45)	0.385 (2)	0.218 (2)	0.626 (2)	4.2 (6)*
C(10)	0.436 (1)	0.304 (2)	0.242 (1)	2.9 (6)	C(46)	0.588 (1)	0.247 (1)	0.728 (1)	2.5 (6)
C(11)	0.375 (2)	0.257 (2)	0.234 (2)	3.6 (5)*	C(47)	0.662 (1)	0.225 (2)	0.754 (2)	3.1 (5)*
C(12)	0.316 (1)	0.273 (2)	0.171 (2)	4.9 (9)	C(48)	0.702 (2)	0.256 (2)	0.827 (2)	4.4 (6)*
C(13)	0.317 (2)	0.388 (2)	0.116 (2)	5 (1)	C(49)	0.679 (1)	0.306 (1)	0.877 (2)	3.6 (7)
C(14)	0.381 (2)	0.384 (2)	0.127 (2)	5.7 (8)*	C(50)	0.607 (2)	0.323 (2)	0.855 (2)	3.7 (7)
C(15)	0.436 (2)	0.363 (2)	0.192 (1)	3.9 (7)	C(51)	0.562 (2)	0.292 (2)	0.778 (2)	4.2 (8)
C(16)	0.589 (2)	0.005 (2)	0.507 (2)	3.9 (8)	Cl(5)	0.2681 (6)	0.0657 (5)	0.2361 (8)	6.5 (3)
C(17)	0.662 (1)	0.008 (2)	0.550 (2)	3.7 (8)	Cl(6)	0.1630 (6)	−0.0331 (7)	0.2716 (7)	7.7 (3)
C(18)	0.713 (2)	−0.050 (2)	0.539 (2)	4.9 (7)*	C(52)	0.179 (1)	0.046 (1)	0.217 (2)	3.8 (8)
C(19)	0.687 (2)	−0.108 (2)	0.485 (2)	5 (1)	C(53)	0.332 (2)	0.753 (3)	0.455 (2)	11.5 (7)*
C(20)	0.611 (2)	−0.113 (2)	0.442 (2)	4.1 (9)	C(54)	0.338 (2)	0.687 (3)	0.408 (2)	11.5 (7)*
C(21)	0.566 (1)	−0.054 (1)	0.453 (2)	3.4 (7)	C(55)	0.398 (2)	0.679 (3)	0.383 (2)	11.5 (7)*
C(22)	0.449 (1)	0.028 (1)	0.522 (1)	2.1 (6)	C(56)	0.453 (2)	0.735 (3)	0.403 (2)	11.5 (7)*
C(23)	0.384 (1)	0.034 (2)	0.457 (2)	3.3 (7)	C(57)	0.447 (2)	0.801 (3)	0.449 (2)	11.5 (7)*
C(24)	0.327 (2)	−0.011 (2)	0.463 (2)	4.7 (7)*	C(58)	0.386 (2)	0.810 (3)	0.475 (2)	11.5 (7)*
C(25)	0.328 (2)	−0.059 (2)	0.527 (2)	5 (1)	O(2)	0.114 (2)	0.510 (2)	0.274 (2)	9.2 (8)*

[a] Starred values denote isotropically refined atoms. Values for anisotropically refined atoms are given in the form of the equivalent isotropic displacement parameter defined as $(4/3)[a^2\beta_{11} + b^2\beta_{22} + c^2\beta_{33} + ab(\cos\gamma)\beta_{12} + ac(\cos\beta)\beta_{13} + bc(\cos\alpha)\beta_{23}]$.

Analogous "A-frame-type" structures have been observed for similar dirhenium $Re_2(L)X_4(dppm)_2$ compounds: L = CO, CNR; X = Cl, Br; R = Me, *t*-Bu, xylyl.[15] While the bond order of the dirhenium compounds is different from that of $Rh_2(CO)Cl_4(dppm)_2$, in both cases π-acceptor ligands are present. Apart from these examples, the A-frame-type geometry is rare for complexes containing an M_2L_9 core. This leads us to propose that the framework of **2** is the thermodynamically favored geometry when one or more ligands are π-acceptors.

Description of the Structure of $[Rh_2(CO)Cl_3(dppm)_2MeOH][PF_6]$ (4). $[Rh_2(CO)Cl_3(dppm)_2MeOH][PF_6]$ has a solid-state structure consisting of a dinuclear metal complex containing an M_2L_9 core. The ORTEP diagram of **4** (Figure 2) reveals a geometry different from that of **2**. The inner coordination sphere is possibly best described as an octahedral environment around Rh(1) sharing an edge with a vertical edge of a square pyramid (C(1) is the apex) around Rh(2). The additional of a second apical ligand (trans to C(1)) would create an octahedral environment around Rh(2). Thus, the geometry could be described as "pre-edge-sharing bioctahedral".

The distance between the two rhodium atoms, 3.010 (2) Å, indicates a weak metal–metal interaction. This weak interaction may be the result of the metal orbitals interacting through p orbitals of the bridging ligands. This interaction is well documented for edge-sharing bioctahedral molecules of the type $M_2Cl_6(PP)_2$ (PP = dmpm, dppm).[16]

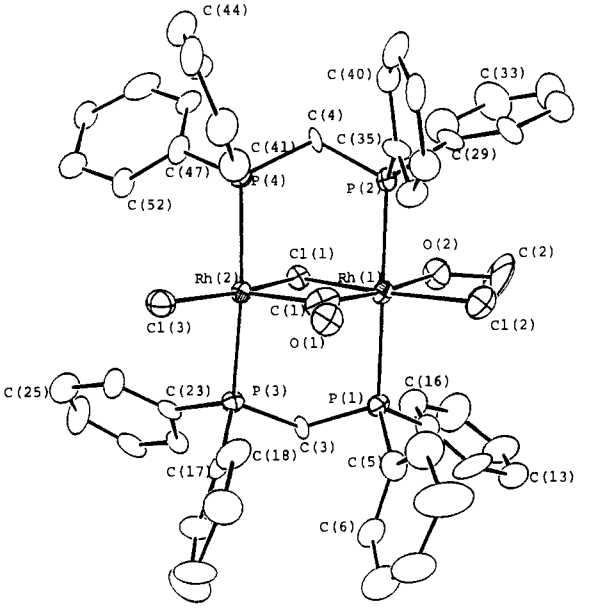

Figure 2. ORTEP diagram of $[Rh_2(CO)Cl_3(dppm)_2MeOH][PF_6]$ (**4**) showing 30% probability ellipsoids. Two carbon atoms of each phenyl ring are labeled. Carbon atoms are numbered sequentially around the ring.

Synthesis and Chemistry of the Dirhodium Compounds. Previous reports indicated that the use of Cl_2 gas in reactions involving $Rh_2(CO)_2Cl_2(dppm)_2$ yielded a variety of uncharacterized products.[4] We observed that addition of $PhICl_2$ to *concentrated* CH_2Cl_2 solutions of $Rh_2(CO)_2Cl_2(dppm)_2$ also led to a variety of uncharacterized products. In contrast, the stepwise addition

(15) (a) Anderson, L. B.; Barder, T. J.; Walton, R. A. *Inorg. Chem.* **1985**, *24*, 1421. (b) Cotton, F. A.; Dunbar, K. R.; Price, A. C.; Schwotzer, W.; Walton, R. A. *J. Am. Chem. Soc.* **1986**, *108*, 4843. (c) Anderson, L. B.; Barder, T. J.; Bursten, B. E.; Esjornson, D.; Walton, R. A. *J. Chem. Soc., Dalton Trans.* **1986**, 2607.

(16) (a) Cotton, F. A.; Chakravarty, A. R.; Diebold, M. P.; Lewis, D. B.; Roth, W. J. *J. Am. Chem. Soc.* **1986**, *108*, 971.

Table III. Positional Parameters and Equivalent Isotropic Thermal Parameters and Their Estimated Standard Deviations for $[Rh_2(CO)Cl_3(dppm)_2MeOH][PF_6]\cdot MeOH$

atom	x	y	z	B,[a] Å²	atom	x	y	z	B,[a] Å²
Rh(1)	0.96345 (8)	0.12357 (5)	0.8916 (1)	2.66 (3)	C(18)	1.215 (1)	0.1723 (7)	0.900 (2)	4.3 (5)
Rh(2)	1.08917 (7)	0.07245 (5)	0.7923 (1)	2.41 (3)	C(19)	1.268 (1)	0.199 (1)	0.956 (2)	5.8 (7)
Cl(1)	0.9832 (2)	0.0852 (2)	0.6852 (4)	2.95 (9)	C(20)	1.308 (1)	0.2327 (8)	0.879 (3)	6.5 (7)
Cl(2)	0.9220 (3)	0.1624 (2)	1.0712 (5)	5.0 (1)	C(21)	1.287 (1)	0.244 (1)	0.754 (2)	7.6 (8)
Cl(3)	1.1991 (3)	0.0506 (2)	0.8571 (5)	4.5 (1)	C(22)	1.235 (1)	0.2140 (8)	0.692 (2)	6.2 (6)
P(1)	1.0049 (3)	0.2003 (2)	0.8087 (4)	2.8 (1)	C(23)	1.1590 (9)	0.1298 (7)	0.537 (1)	2.7 (4)
P(2)	0.9259 (2)	0.0482 (2)	0.9799 (4)	2.5 (1)	C(24)	1.199 (1)	0.0906 (7)	0.515 (2)	3.5 (5)
P(3)	1.1296 (2)	0.1445 (2)	0.6946 (4)	2.5 (1)	C(25)	1.225 (1)	0.0765 (8)	0.397 (2)	5.1 (5)
P(4)	1.0456 (3)	−0.0051 (2)	0.8525 (4)	2.5 (1)	C(26)	1.198 (1)	0.1027 (8)	0.291 (2)	5.2 (6)
P(5)	0.6367 (4)	0.1542 (3)	0.5030 (8)	6.9 (2)	C(27)	1.160 (1)	0.1453 (8)	0.306 (2)	4.9 (5)
F(1)	0.607 (1)	0.2045 (8)	0.487 (2)	12.0 (6)*	C(28)	1.1386 (9)	0.1582 (6)	0.428 (1)	2.6 (4)
F(2)	0.581 (1)	0.1405 (9)	0.601 (3)	15.3 (8)*	C(29)	0.8329 (9)	0.0443 (7)	0.992 (2)	3.2 (4)
F(3)	0.675 (1)	0.101 (1)	0.519 (3)	15.9 (8)*	C(30)	0.802 (1)	0.0587 (7)	1.105 (2)	4.1 (5)
F(4)	0.695 (1)	0.1677 (8)	0.405 (2)	13.4 (6)*	C(31)	0.730 (1)	0.0605 (8)	1.111 (2)	5.1 (6)
F(5)	0.590 (2)	0.133 (1)	0.403 (4)	22 (1)*	C(32)	0.690 (1)	0.048 (1)	1.012 (3)	6.8 (8)
F(6)	0.684 (2)	0.168 (1)	0.615 (3)	17.9 (9)*	C(33)	0.721 (1)	0.033 (1)	0.901 (3)	7.4 (8)
O(1)	1.0893 (8)	0.1169 (5)	1.040 (1)	4.7 (3)	C(34)	0.794 (1)	0.032 (1)	0.886 (3)	7.2 (6)*
O(2)	0.8591 (7)	0.1343 (5)	0.806 (1)	5.1 (4)	C(35)	0.9559 (9)	0.0312 (6)	1.138 (2)	3.1 (4)
O(3)	0.818 (2)	0.096 (1)	0.574 (3)	14.6 (9)*	C(36)	0.991 (1)	0.0643 (6)	1.214 (2)	3.5 (4)
C(1)	1.056 (1)	0.1064 (7)	0.950 (2)	4.1 (5)	C(37)	1.010 (1)	0.0498 (7)	1.340 (1)	3.7 (5)
C(2)	0.801 (2)	0.160 (1)	0.845 (4)	13 (1)	C(38)	0.996 (1)	0.0022 (7)	1.379 (2)	4.2 (5)
C(3)	1.0600 (8)	0.1903 (6)	0.668 (2)	3.2 (4)	C(39)	0.965 (1)	−0.0314 (7)	1.302 (2)	4.3 (5)
C(4)	0.9511 (9)	−0.0039 (6)	0.884 (2)	3.3 (4)	C(40)	0.942 (1)	−0.0178 (7)	1.182 (2)	4.2 (5)
C(5)	1.055 (1)	0.2415 (7)	0.911 (2)	3.4 (4)	C(41)	1.0834 (9)	−0.0385 (6)	0.984 (1)	2.1 (4)
C(6)	1.096 (1)	0.2795 (8)	0.846 (2)	5.9 (6)	C(42)	1.119 (1)	−0.0126 (7)	1.080 (2)	4.0 (5)
C(7)	1.137 (1)	0.310 (1)	0.925 (4)	9 (1)	C(43)	1.146 (1)	−0.0389 (8)	1.187 (2)	4.7 (5)
C(8)	1.134 (2)	0.304 (1)	1.055 (3)	6.9 (8)	C(44)	1.140 (1)	−0.0923 (8)	1.184 (2)	4.2 (5)
C(9)	1.089 (2)	0.270 (1)	1.122 (3)	10 (1)	C(45)	1.107 (1)	−0.1162 (8)	1.093 (2)	5.4 (6)
C(10)	1.056 (1)	0.2367 (9)	1.041 (2)	6.5 (7)	C(46)	1.077 (1)	−0.0902 (7)	0.992 (2)	4.1 (5)
C(11)	0.939 (1)	0.2386 (7)	0.743 (2)	3.4 (4)	C(47)	1.056 (1)	−0.0471 (6)	0.716 (2)	3.2 (4)
C(12)	0.923 (1)	0.2824 (6)	0.783 (2)	4.8 (5)	C(48)	1.006 (1)	−0.0777 (6)	0.675 (2)	3.2 (4)
C(13)	0.865 (1)	0.3096 (7)	0.742 (2)	5.6 (6)	C(49)	1.018 (2)	−0.1080 (7)	0.573 (2)	6.0 (7)
C(14)	0.827 (2)	0.2927 (8)	0.638 (2)	6.5 (7)	C(50)	1.078 (1)	−0.1083 (7)	0.506 (1)	3.6 (5)
C(15)	0.845 (2)	0.2480 (9)	0.587 (2)	6.9 (7)	C(51)	1.133 (1)	−0.0760 (7)	0.549 (2)	4.3 (5)
C(16)	0.906 (1)	0.2217 (7)	0.637 (2)	4.5 (5)	C(52)	1.117 (1)	−0.0441 (7)	0.655 (2)	4.0 (5)
C(17)	1.199 (1)	0.1792 (6)	0.769 (2)	3.1 (4)	C(53)	0.846 (3)	0.101 (2)	0.440 (5)	16 (2)*

[a] Starred values denote isotropically refined atoms. Values for anisotropically refined atoms are given in the form of the equivalent isotropic displacement parameter defined as $(4/3)[a^2\beta_{11} + b^2\beta_{22} + c^2\beta_{33} + ab(\cos\gamma)\beta_{12} + ac(\cos\beta)\beta_{13} + bc(\cos\alpha)\beta_{23}]$.

Table IV. Selected Bond Distances (Å) and Bond Angles (deg) for $Rh_2(CO)Cl_4(dppm)_2\cdot CH_2Cl_2\cdot C_6H_6\cdot H_2O$[a]

Distances

Rh(1)–Rh(2)	2.691 (3)	Rh(2)–Cl(3)	2.373 (8)
Rh(1)–Cl(1)	2.448 (7)	Rh(2)–Cl(4)	2.430 (9)
Rh(1)–Cl(2)	2.384 (7)	Rh(2)–P(3)	2.342 (8)
Rh(1)–P(1)	2.361 (8)	Rh(2)–P(4)	2.331 (8)
Rh(1)–P(2)	2.349 (8)	P(1)–C(2)	1.85 (3)
Rh(1)–C(1)	1.83 (3)	O(1)–C(1)	1.10 (4)
Rh(2)–Cl(2)	2.399 (6)		

Angles

Rh(2)–Rh(1)–Cl(1)	160.3 (2)	Rh(1)–Rh(2)–Cl(4)	162.6 (2)
Rh(2)–Rh(1)–Cl(2)	56.0 (2)	Rh(1)–Rh(2)–P(3)	94.7 (2)
Rh(2)–Rh(1)–P(1)	92.4 (2)	Rh(1)–Rh(2)–P(4)	94.1 (2)
Rh(2)–Rh(1)–P(2)	93.5 (2)	Cl(2)–Rh(2)–Cl(3)	150.9 (3)
Rh(2)–Rh(1)–C(1)	102.3 (9)	Cl(2)–Rh(2)–Cl(4)	107.1 (3)
Cl(1)–Rh(1)–Cl(2)	104.4 (2)	Cl(2)–Rh(2)–P(3)	95.2 (3)
Cl(1)–Rh(1)–P(1)	87.4 (3)	Cl(2)–Rh(2)–P(4)	94.7 (3)
Cl(1)–Rh(1)–P(2)	89.3 (3)	Cl(3)–Rh(2)–Cl(4)	102.0 (3)
Cl(1)–Rh(1)–C(1)	97.3 (9)	Cl(3)–Rh(2)–P(3)	86.1 (3)
Cl(2)–Rh(1)–P(1)	95.5 (3)	Cl(3)–Rh(2)–P(4)	87.2 (3)
Cl(2)–Rh(1)–P(2)	93.6 (3)	Cl(4)–Rh(2)–P(3)	86.4 (3)
Cl(2)–Rh(1)–C(1)	158.0 (9)	Cl(4)–Rh(2)–P(4)	86.9 (3)
P(1)–Rh(1)–P(2)	170.9 (3)	P(3)–Rh(2)–P(4)	169.3 (3)
P(1)–Rh(1)–C(1)	89 (1)	Rh(1)–Cl(2)–Rh(2)	68.5 (2)
P(2)–Rh(1)–C(1)	83 (1)	Rh(1)–P(1)–C(2)	113.5 (9)
Rh(1)–Rh(2)–Cl(2)	55.5 (2)	Rh(1)–C(1)–O(1)	172 (3)
Rh(1)–Rh(2)–Cl(3)	95.4 (2)		

[a] Numbers in parentheses are estimated standard deviations in the least significant digits.

of $PhICl_2$ to *dilute* CH_2Cl_2 solutions of $Rh_2(CO)_2Cl_2(dppm)_2$ yields products that have been characterized by solution and solid-state methods. One equivalent of $PhICl_2$ reacts with $Rh_2(CO)_2Cl_2(dppm)_2$ to yield the dicarbonyl $Rh_2(CO)_2Cl_4(dppm)_2$ (**1**), which was characterized by IR and $^{31}P\{^1H\}$ NMR spectroscopies.

The initial solution IR spectrum, measured during the first 5 min of the reaction, revealed three carbonyl peaks at 2047, 2023 and 1990 cm^{-1}. We have attributed the latter band to unreacted $Rh_2(CO)_2Cl_2(dppm)_2$ while the bands at 2047 and 2023 cm^{-1} are due to compounds **1** and **2**, respectively. During the course of the reaction, the bands at 2047 and 1990 cm^{-1} slowly decreased in intensity while that at 2023 cm^{-1} increased. After a few hours the only band remaining was that at 2023 cm^{-1}. This is good evidence that the dicarbonyl, **1**, is formed as an intermediate and decarbonylates to the monocarbonyl, **2**, in solution (Scheme I). To verify that this process is reversible, we passed CO through a CH_2Cl_2 solution of **2**. The IR spectrum of the resulting orange solution revealed only the band at 2047 cm^{-1}; i.e., **1** had been re-formed. This solution quickly changed color back to dark orange-brown on exposure to the atmosphere for a few minutes and exhibited a weak band at 2047 cm^{-1} (for **1**) and a much stronger band at 2023 cm^{-1} (for **2**) in its IR spectrum.

The $^{31}P\{^1H\}$ NMR spectrum of **1** (measured on a CH_2Cl_2 solution that was prepared by passing CO through **2** and retaining an atmosphere of CO in the NMR tube) reveals a AA'A''A'''XX' pattern (Figure 3a), indicating that the complex is symmetrical. The structure of **1** is most likely analogous to that proposed[3] for $Rh_2(CO)_2Cl_2I_2(dppm)_2$ (I). An edge-sharing bioctahedral

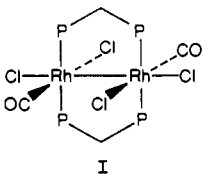

I

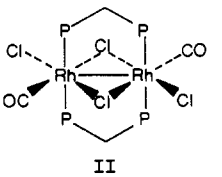

II

Table V. Selected Bond Distances (Å) and Bond Angles (deg) for $[Rh_2(CO)Cl_3(dppm)_2MeOH][PF_6]\cdot MeOH$[a]

	Distances		
Rh(1)–Rh(2)	3.010 (2)	P(1)–C(3)	1.85 (2)
Rh(1)–Cl(1)	2.440 (4)	P(2)–C(4)	1.80 (2)
Rh(1)–Cl(2)	2.311 (5)	P(5)–F(1)	1.49 (2)
Rh(1)–P(1)	2.393 (4)	P(5)–F(2)	1.55 (3)
Rh(1)–P(2)	2.357 (5)	P(5)–F(3)	1.63 (3)
Rh(1)–O(2)	2.249 (13)	P(5)–F(4)	1.58 (3)
Rh(1)–C(1)	1.97 (2)	P(5)–F(5)	1.51 (4)
Rh(2)–Cl(1)	2.387 (5)	P(5)–F(6)	1.54 (3)
Rh(2)–Cl(3)	2.334 (6)	O(1)–C(1)	1.18 (2)
Rh(2)–P(3)	2.342 (4)	O(2)–C(2)	1.39 (4)
Rh(2)–P(4)	2.351 (4)	O(3)–C(53)	1.52 (6)
Rh(2)–C(1)	2.00 (2)		
	Angles		
Cl(1)–Rh(1)–P(1)	89.4 (2)	Cl(3)–Rh(2)–P(4)	91.7 (2)
Cl(1)–Rh(1)–P(2)	91.9 (2)	Cl(3)–Rh(2)–C(1)	100.0 (6)
Cl(1)–Rh(1)–O(2)	81.0 (4)	P(3)–Rh(2)–P(4)	169.6 (2)
Cl(1)–Rh(1)–C(1)	91.8 (5)	P(3)–Rh(2)–C(1)	95.2 (5)
Cl(2)–Rh(1)–P(1)	91.4 (2)	P(4)–Rh(2)–C(1)	94.0 (6)
Cl(2)–Rh(1)–P(2)	87.7 (2)	Rh(1)–Cl(1)–Rh(2)	77.2 (1)
Cl(2)–Rh(1)–O(2)	87.1 (4)	Rh(1)–P(2)–C(4)	111.8 (6)
Cl(2)–Rh(1)–C(1)	100.1 (5)	F(1)–P(5)–F(2)	91 (1)
P(1)–Rh(1)–P(2)	177.7 (2)	F(1)–P(5)–F(3)	176 (1)
P(1)–Rh(1)–O(2)	92.9 (4)	F(1)–P(5)–F(4)	89 (1)
P(1)–Rh(1)–C(1)	90.3 (6)	F(1)–P(5)–F(5)	92 (2)
P(2)–Rh(1)–O(2)	89.2 (4)	F(1)–P(5)–F(6)	96 (1)
O(2)–Rh(1)–C(1)	172.1 (6)	Rh(1)–O(2)–C(2)	133 (2)
Cl(1)–Rh(2)–Cl(3)	167.5 (2)	Rh(1)–C(1)–Rh(2)	98.6 (8)
Cl(1)–Rh(2)–P(3)	88.0 (2)	Rh(1)–C(1)–O(1)	134 (2)
Cl(1)–Rh(2)–P(4)	86.6 (2)	Rh(2)–C(1)–O(1)	126 (2)
Cl(1)–Rh(2)–C(1)	92.5 (6)	P(1)–C(3)–P(3)	114 (1)
Cl(3)–Rh(2)–P(3)	91.6 (2)	P(2)–C(4)–P(4)	112.5 (9)

[a] Numbers in parentheses are estimated standard deviations in the least significant digits.

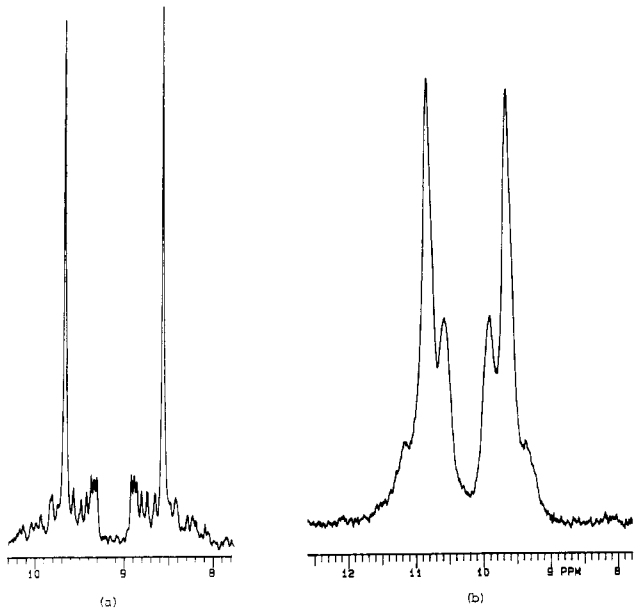

Figure 3. $^{31}P\{^1H\}$ NMR spectra: (a) $Rh_2(CO)_2Cl_4(dppm)_2$ (**1**); (b) $[Rh_2(CO)Cl_3(dppm)_2][Cl]$.

structure (II) would appear to require 19 (no Rh–Rh bond) or 20 (Rh–Rh bond) electron configurations at the metal atoms and is, therefore, less likely.

The size of the rhodium–phosphorus coupling constant, 104.9 Hz, is consistent with that of a dimeric rhodium complex containing a Rh–Rh bond.[17] Determination of the extent of the metal–metal interaction necessitates crystallographic analysis. Crystallization of $Rh_2(CO)_2Cl_4(dppm)_2$ (**1**) has not been accomplished because of decarbonylation of $Rh_2(CO)_2Cl_4(dppm)_2$ in solution to form $Rh_2(CO)Cl_4(dppm)_2$. The rate of $Rh_2(CO)_2Cl_4(dppm)_2$ decarbonylation is increased with the addition of one equivalent of $PhICl_2$ to a CH_2Cl_2 solution of the metal complex. The products of this reaction were analyzed by IR and $^{31}P\{^1H\}$ NMR spectroscopies and were shown to be a mixture of $Rh_2(CO)Cl_4(dppm)_2$ and $Rh_2Cl_6(dppm)_2$. We initially postulated that Cl_2CO formation might facilitate a more rapid shift in the equilibrium of the reaction to form $Rh_2(CO)_2Cl_4(dppm)_2$. We tested this by allowing the effluent gas from the reaction of $Rh_2(CO)_2Cl_4(dppm)_2$ with $PhICl_2$ to pass through methanol. The methanol was later analyzed by $^{13}C\{^1H\}$ NMR spectroscopy for the presence of $(MeO)_2CO$, but no peaks attributable to $(MeO)_2CO$ were found. Presumably the speed of the reaction increases simply because of an increase in $PhICl_2$ according to a simple bimolecular rate law: $k = [PhICl_2][Rh_2(CO)_2Cl_4(dppm)_2]$.

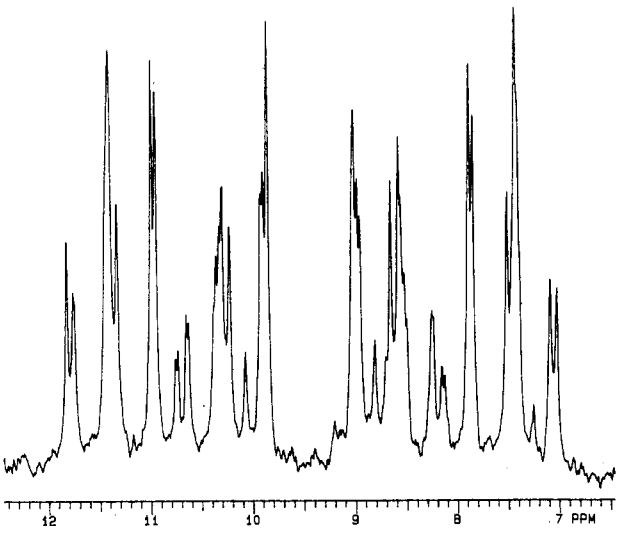

Figure 4. $^{31}P\{^1H\}$ NMR spectrum of $Rh_2(CO)Cl_4(dppm)_2$ (**2**).

$Rh_2(CO)Cl_4(dppm)_2$ (**2**) is best formed by the 4-day decarbonylation reaction of $Rh_2(CO)_2Cl_4(dppm)_2$. Compound **2** exhibits one CO stretching band in both the solution (ν = 2023 cm^{-1}) and in the solid (ν = 2022 cm^{-1}) IR spectra, and the $^{31}P\{^1H\}$ NMR spectrum of 200 MHz (Figure 4) shows a complex AA'BB' pattern with two distinct phosphorus chemical shifts, centered at 8.1 and 10.9 ppm. Clearly, the phosphorus nuclei are reporting different environments about the two rhodium atoms, consistent with the presence of a therminal rather than a bridging CO ligand. Crystals of **2**, when redissolved in CH_2Cl_2, give the same solution spectrum observed in Figure 4. A 200-MHz spectrometer has allowed unambiguous observation of two chemical shifts, whereas the 90-MHz spectrometer used by Woods et al.[4] could not do so.

The reaction of **2** with 1 equiv of $PhICl_2$ proceeds in a straightforward manner to give the highly oxidized product $Rh_2Cl_6(dppm)_2$ (**3**). The IR spectrum is devoid of a CO stretching band, as expected. The $^{31}P\{^1H\}$ NMR spectrum is an AX pattern centered at δ = 4.65, with $^1J_{Rh-P}$ = 85.5 Hz, indicative of a symmetrical environment around the dimetal core. Details of the structure of **3** will be the subject of a future publication.

All three oxidation products, $Rh_2(CO)_2Cl_4(dppm)_2$ (**1**), $Rh_2(CO)Cl_4(dppm)_2$ (**2**), and $Rh_2Cl_6(dppm)_2$ (**3**) were shown to be air-stable by exposing samples to air and then examining them by IR and $^{31}P\{^1H\}$ NMR spectroscopies. $Rh_2(CO)_2Cl_4(dppm)_2$ decarbonylates with time under an inert atmosphere and in the air.

The synthesis of **2**, by either method 1 or 2, does not yield pure $Rh_2(CO)Cl_4(dppm)_2$. Method 1 leaves trace amounts of $Rh_2(CO)_2Cl_4(dppm)_2$, even after a 4-day reaction time. Method 2 produces small amounts of $Rh_2Cl_6(dppm)_2$ while trace amounts of $Rh_2(CO)_2Cl_4(dppm)_2$ remain unreacted. Mixtures of $Rh_2(CO)_2Cl_4(dppm)_2$, $Rh_2(CO)Cl_4(dppm)_2$, and $Rh_2Cl_6(dppm)_2$ are

(17) (a) Cowie, M.; Dickson, R. S.; Hames, B. W. *Organometallics* **1984**, *3*, 1879. (b) Cowie, M.; Dwight, S. K. *Inorg. Chem.* **1980**, *19*, 209. (c) Balch, A. L. *Homogeneous Catalysis with Metal Phosphine Complexes*; Pignolet, L. G.; Ed.; Plenum: New York, 1984; Chapter 5.

cleanly separated by flash column chromatography.[8] The compounds are eluted in the following order: $Rh_2Cl_6(dppm)_2$, $Rh_2(CO)Cl_4(dppm)_2$, and $Rh_2(CO)_2Cl_4(dppm)_2$.

$Rh_2(CO)Cl_4(dppm)_2$ undergoes a variety of reactions, of which a small number will be discussed. A brown CH_2Cl_2 solution of $Rh_2(CO)Cl_4(dppm)_2$ turns green upon the addition of methanol. A $^{31}P\{^1H\}$ NMR spectrum of the solution (Figure 3b) reveals an AA'A''A'''XX' pattern, indicating the formation of a symmetrical compound. The AA'A''A'''XX' pattern and the size of the rhodium–phosphorus coupling constant, 94.6 Hz, are indicative of a Rh–Rh bond. This reaction is reversed when MeOH is removed.

A more permanent transformation to the symmetric species is effected when a CH_2Cl_2 solution of **2** is treated with $AgPF_6$. The green compound, $[Rh_2(CO)Cl_3(dppm)_2][PF_6]$, can be isolated in essentially quantitative yield, and also as a methanol adduct (compound **4**). The $^{31}P\{^1H\}$ NMR spectrum of a CH_2Cl_2 solution of this compound, is essentially the same as that shown in Figure 3b. The solution IR spectrum reveals a band at $\nu = 1790$ cm^{-1}, consistent with the presence of a bridging CO ligand in the complex, namely

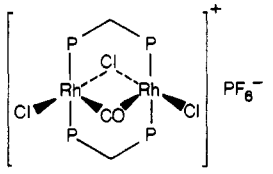

Reactions of **2** with $BF_3{\cdot}Et_2O$ and $NaBPh_4$ yield the same cation. The latter two reagents react faster in $MeOH/CH_2Cl_2$ solutions of **2**, presumably because MeOH facilitates initial chloride dissociation, and the larger, noncoordinating anion replaces Cl^-. Crystals of the PF_6 complex, **4**, were grown from $MeOH/CH_2Cl_2$. The solid structure reveals a coordinated methanol solvent molecule. If the solid structure persisted in solution, a complex $^{31}P\{^1H\}$ NMR pattern would have been observed, instead of the simple one discussed above. Crystals of **4**, redissolved in CH_2Cl_2, give the same $^{31}P\{^1H\}$ NMR pattern as shown in Figure 3b. Thus, the MeOH that is coordinated in the crystal of **4** does not remain associated with the complex in solution. The spectrum we observe for our rhodium cation is consistent with that reported by Woods et al.[4]

The carbonyl ligand of **2** may be removed under controlled conditions by the addition of Me_3NO. (Note that a mild decarbonylation reagent, $BF_3{\cdot}Et_2O$, yielded only the dirhodium cation.) At room temperature, Me_3NO causes decomposition of **2**; the only product detected by $^{31}P\{^1H\}$ NMR spectroscopy is bis(diphenylphosphino)methane oxide. At −72 °C, the decarbonylation reaction proceeds faster than dimer decomposition, thus affording good yields of $Rh_2Cl_4(dppm)_2$ (**5**). The geometric rearrangement of the phosphine ligands around the rhodium–rhodium vector from transoid in **2** to cisoid in **5** may account for the difficulty in decarbonylating **2**. Compound **5** was previously prepared by the reaction of $Rh_2(O_2CCH_3)_4$ with 2 equiv of dppm and 4 equiv of Me_3SiCl.[6]

Under the forceful reaction condition of 200 psi of CO, $Rh_2Cl_4(dppm)_2$ slowly reacts to form $Rh_2(CO)Cl_4(dppm)_2$ (**2**). $Rh_2(CO)_2Cl_4(dppm)_2$ also forms from this reaction, indicating that carbonylation of **5** is the difficult step. Bubbling CO through a CH_2Cl_2 slurry of $Rh_2Cl_4(dppm)_2$ does not lead to a reaction.

Attempts to find suitable conditions to form $Rh_2Cl_6(dppm)_2$ from $Rh_2Cl_4(dppm)_2$ in Cl_2 (liquid) led only to uncharacterized products. Again, the cisoid to transoid rearrangement of phosphines about the Rh–Rh vector can probably be cited as the principal impediment to the reaction, especially in view of the facile reaction of **2** to form **3** where such a geometrical rearrangement is not necessitated.

Acknowledgment. We thank the National Science Foundation for financial support and Steven K. Silber of this department for helpful discussions regarding $^{31}P\{^1H\}$ NMR spectroscopy. We are also grateful to Dr. R. Poli for useful discussions and assistance at the outset.

Supplementary Material Available: For the crystal structures of **2** and **4**, full tables of crystal parameters and details of data collection and refinement, bond distances, bond angles, and anisotropic displacement parameters (34 pages); tables of observed and calculated structure factors (34 pages). Ordering information is given on any current masthead page.

Contribution from the Department of Chemistry and Laboratory for Molecular Structure and Bonding, Texas A&M University, College Station, Texas 77843

Oxidation States Available to the Ru_2^{n+} Core in Tetracarboxylato-Bridged Species

F. Albert Cotton,* Marek Matusz, and Bianxiao Zhong

Received June 3, 1988

Prompted by reports of the preparation and properties of two $Ru_2(O_2CR)_4^{2+}$ type compounds, we prepared a diruthenium propionate (**1**) by using the method given for the two alleged $Ru_2(O_2CR)_4^{2+}$ compounds. The crystal structure study of **1** showed that it was $Ru_2(O_2CCH_2CH_3)_5$, instead of $Ru_2(O_2CCH_2CH_3)_6$. This led us to reinvestigate the two previously described substances. A reanalysis of the structure data for a reported $Ru_2(O_2CCH_3)_6{\cdot}0.7H_2O$ compound, as well as measurements of its spectral, electrochemical and magnetic properties indicated that it was actually $Ru_2(O_2CCH_3)_4{\cdot}(CH_3CO_2)_2H{\cdot}0.7H_2O$ (**3**). A crystal structure study revealed that another type of compound obtained by the reported method was actually $Ru_2(O_2CCF_3)_5$ (**2**). Our work shows that so far there is no evidence for the existence of $Ru_2(O_2CR)_4^{2+}$ type complexes. Crystal data for new compounds are as follows. **1**: space group $P2_12_12_1$; $a = 13.843$ (3) Å, $b = 17.189$ (5) Å, $c = 8.758$ (1) Å, $V = 2084.0$ (8) Å^3, $Z = 4$. **2**: space group $C2/c$; $a = 12.628$ (5) Å, $b = 11.771$ (5) Å, $c = 13.563$ (4) Å, $\beta = 106.98$ (4)°, $V = 1928$ (2) Å^3, $Z = 4$.

Introduction

The existence of Ru–Ru multiple bonding was first recognized in the compound $Ru_2(O_2CC_3H_7)_4Cl$ in 1969[1] although the preparation of this and similar compounds had been reported several years earlier.[2] The first detailed examination of the magnetic and redox properties of this compound was reported only in 1975,[3] and it was not until 1979 that a detailed theoretical study appeared.[4] The voltammetric study of redox properties showed that reduction occurs in the range 0.00 to −0.34 V (vs SCE), with

(1) Bennett, M. J.; Caulton, K. G.; Cotton, F. A. *Inorg. Chem.* **1969**, *8*, 1.
(2) Stephenson, T. A.; Wilkinson, G. *J. Inorg. Nucl. Chem.* **1966**, *28*, 2285.
(3) Cotton, F. A.; Pedersen, E. *Inorg. Chem.* **1975**, *14*, 388.
(4) Norman, J. G.; Renzoni, G. E.; Case, D. A. *J. Am. Chem. Soc.* **1979**, *101*, 5256.

0020-1669/88/1327-4368$01.50/0